Agro-Ecosystem Informatics for Rational Crop and Field Management
– Remote Sensing, GIS and Modeling –

Yoshio INOUE

National Institute for Agro-Environmental Sciences

3-1-3, Kan-non-dai, Tsukuba, Ibaraki, 305-8604, Japan

E-mail: yinoue@niaes.affrc.go.jp

Abstract: Spatial and timely information on crop and filed conditions is one of the most important basics for rational and efficient planning and management in agriculture. Remote sensing, GIS, and modeling are powerful tools for such applications. This paper presents an overview of the state of the art in remote sensing of crop and field conditions with some case studies. It is also shown that a synergistic linkage between process-based models and remote sensing signatures enables us to estimate the multiple crop/ecosystem variables at a dynamic mode. Remotely sensed information can greatly reduce the uncertainty of simulation models by compensating for insufficient availability of data or parameters. This synergistic approach allows the effective use of infrequent and multi-source remote sensing data for estimating important ecosystem variables such as biomass growth and ecosystem CO_2 flux. This paper also shows a geo-spatial information system that enables us to integrate, search, extract, process, transform, and calculate any part of the data based on ID#, attributes, and/or by river-basin boundary, administrative boundary, or boundaries of arbitrary shape/size all over Japan. A case study using the system demonstrates that the nitrogen load from fertilizer was closely related to nitrate concentration of groundwater. The combined use of remote sensing, GIS and modeling would have great potential for various agro-ecosystem applications.

Keywords: agro-chemicals, assessment, GIS, informatics, precision farming, pollution, process model, productivity, remote sensing, site specific management, simulation, synergy.

1. Introduction – background & research needs –

The efficient use of resources such as soil, water, energy, and agro-chemicals is one of the most important aspects of precision agriculture. This is the basis for cost reduction and less negative impact on

environment. Therefore, it is often required to understand and assess the environmental impacts at landscape, catchment-area, or regional scales.

Remote sensing is the powerful tool for acquisition of such information in a wide range of applications (Moran and Inoue, 1997). Bio-physical signatures over the broad electromagnetic domains (optical, thermal and microwave) can be detected on remote/non-destructive, wide-area, and real-time basis. Within-field or between-field differences can be assessed efficiently by remote sensing. On the other hand process-based modeling allows dynamic assessment/prediction of crop and field conditions. Nevertheless, both methods have some inherent limitations, respectively (Inoue and Olioso, 2004a). Thus, this paper reviews and analyze the state of the art in remote sensing of crop and field conditions, and to investigate the potential of a new approach which combine remote sensing and process-based modeling.

Another useful tool is GIS (geographical information system). Since every piece of farmland has different topographic, climatic, soil, and management conditions, and these properties affect the crop productivity and environmental impacts of agriculture at larger scales. Thus, a generic information system should be crucial for systematic integration and analysis of geo-spatial data and information at a fine scale of farmland. In this paper, a case study on development and application of geo-spatial information system is demonstrated.

2. Remote Sensing of Crop and Field – an overview –

2.1 Sensors and platforms for precision farming

A range of platforms and sensor systems can be used for remote sensing of crop/field for precision farming; optical, thermal, and microwave sensors are available for space-borne, airborne, and ground-based platforms (see review by Moran and Inoue, 1997; Inoue, 1998; Inoue et al., 2000; Inoue 2003; Inoue and Olioso, 2004a). The application of remote sensing to precision crop management involves at least three important requirements: (1) electromagnetic features, (2) spatial resolution, and (3) temporal resolution (Moran and Inoue, 1997). Hyperspectral signature may be useful for detection of biotic and abiotic plant stresses (Inoue, 1998). One of the most attractive aspects of active microwave signature is to permeate through clouds. Thermal signature is useful especially for detection of water stress and for calculation of energy balance. Spatial resolution is important in applications in precision crop management; 1m resolution on the ground is optimal for various purposes which is already available from some satellite sensors. High temporal resolution such as 1 week is also required for growth monitoring although cloudy conditions often hamper the observation by optical sensors. Details can be found in the above review papers.

23

2.2 Relationships useful for diagnosis and prediction of crop and field conditions

Figure 1 depicts the hyper-spectra for various targets in agro-ecosystems. Hereafter, spectral ranges in visible, near-infrared, and shortwave-infrared are expressed as VIS, NIR and SWIR, respectively; the spectral reflectance at ### nm is expressed as ρ### (e.g., spectral reflectance at 850 nm is ρ850). A wide range of soil, crop parameters can be estimated from remotely sensed information. In this paper, due to page limitation, some of results mainly from our research studies are presented. More detailed information can be found in reviews by Moran and Inoue (1997), Inoue (2003), and Inoue and Olioso (2004a).

2.2.1 Biomass, leaf area index LAI, and Yield

Broad band signatures in VIS and NIR are useful for estimating green biomass or LAI, and a considerable number of spectral indices such as NDVI (= $[\rho_{NIR}-\rho_{RED}]/[\rho_{NIR}+\rho_{RED}]$; ρ_{NIR} and ρ_{RED} are reflectance at near-infrared and red wavelengths) have been proposed (see a review by Inoue and Olioso, 2004a) Recently, we also found that microwave backscattering signatures in L-band (1.26 GHz) and C band (5.75 GHz) are promising in estimation of biomass and LAI, respectively (Figure 2; Inoue et al., 2002). A number of attempts have been made to correlate remotely sensed signatures with the final yield of various crops (e.g., wheat, maize, rice, soybean, barley, sugar beet). The NDVI at critical growth stages such as heading, and the temporal integral of such indices over specific periods, have been correlated to final yield (e.g., Rasmussen, 1992). These are all based on the correlation between above-ground biomass at some stage and final yield. Since senescence during maturity and the duration of the grain filling period are also related to changes in NDVI, the index is correlated with the final yield (e.g., Potdar, 1993). Grain yield at maturity can be estimated by spectral reflectance within the 500- to 700-nm and 900- to 1300-nm wavelength regions (Shibayama et al., 1991), and at 1100 and 1650 nm (Inoue et al., 1998). Remotely
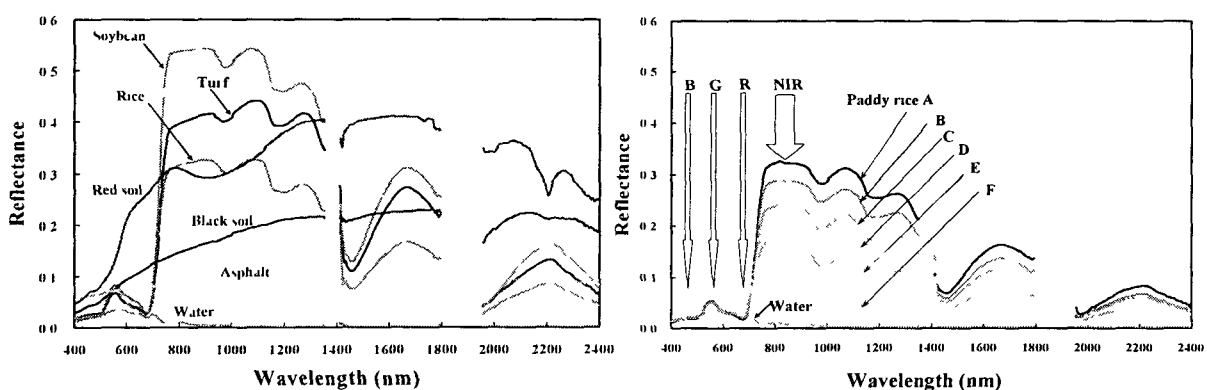

Fig.1. Typical spectra for agro-ecosystem surfaces, and for paddy fields at different conditions. (Inoue et al., 2001)
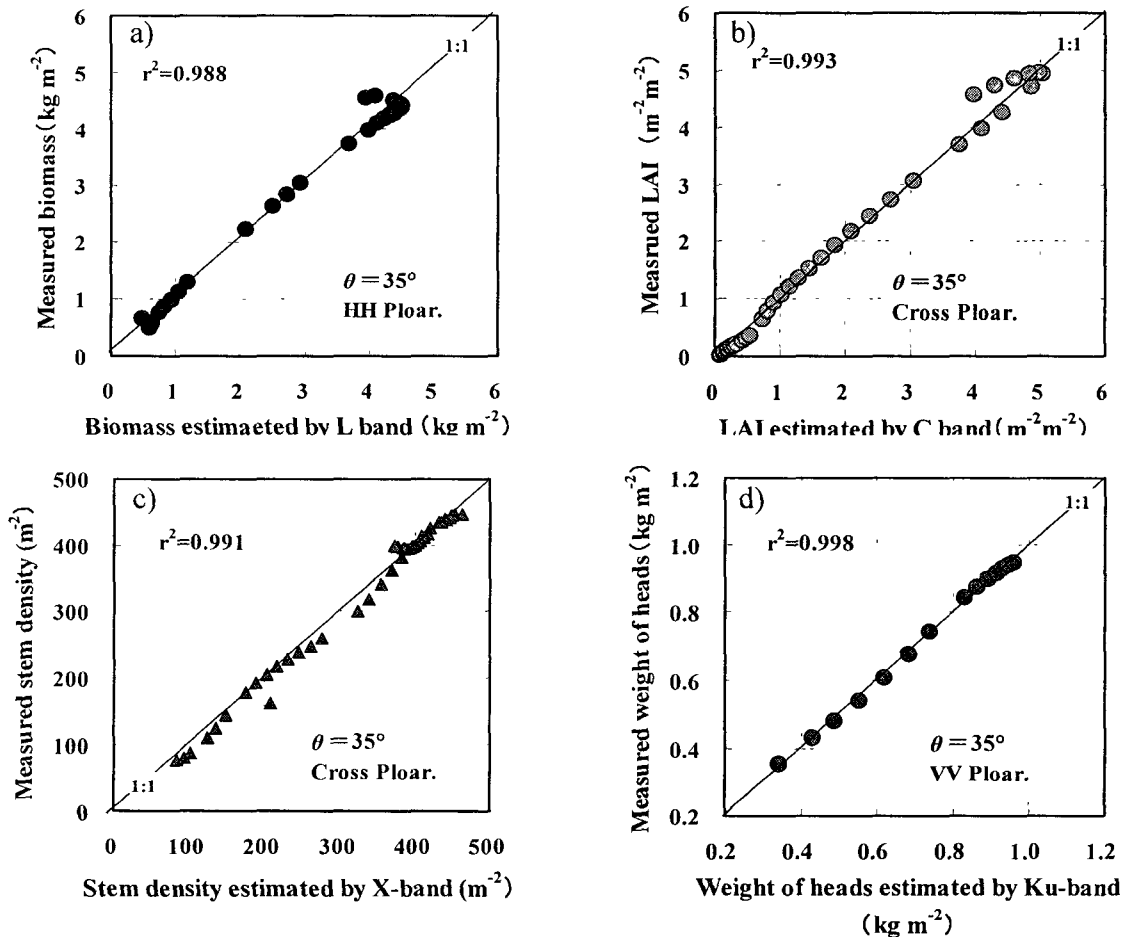
24

Fig. 2. Comparison between canopy variables measured by destructive sampling and estimated by backscattering coefficients in different frequency; a) Biomass, b) LAI c) stem density, and d) weight of heads, respectively. (Inoue et al., 2002)

sensed surface temperature was also related to yield using stress-degree-days (Idso et al., 1980). Since leaf temperature is closely related to water stress, the sum of the canopy-air temperature differences (stress-degree-days) during the grain filling period is correlated with the final yield (Seguin et al., 1989). Other data that are useful for yield forecasting can be obtained from microwave backscattering signatures, because the C-band (5 GHz) and L-band (1.5 GHz) are related to biomass, as noted in the previous section. The close relation found between weight of rice heads and backscattering coefficients in the Ka-band (35 GHz) and the Ku-band (16 GHz) may provide useful information about the growth of heads during the grain filling period (Inoue et al., 2002). In general, these correlations should be used very carefully

because the applicability of regression models is strongly affected by the range of the data set, even when the correlations are real correlations based on mechanistic foundations. These regression approaches are usually simple in terms of both model structure and data requirements, but model parameters must be determined for each crop, variety, location, and other variables.

2.2.2 Chlorophyll, Nitrogen and Water Contents

These three variables can be estimated from hyperspectral measurements over VIS, NIR and SWIR wavelengths. Figure 3 shows that chlorophyll concentration in leaves of rice canopies can be estimated using a few hyper spectral bands in visible and NIR wavelengths, which was obtained by a hyperspectral imager developed by the authors (Inoue and Peñuelas, 2001). A simple index $\rho830/\rho550$ is also useful for estimating nitrogen concentration of rice canopy with the similar mass of leaves (Figure 4), which is useful for diagnosis of maturity and protein content of grain. Total amount of canopy nitrogen can be estimated by using 4 broad bands in VIS, NIR and SWIR bands (Figure 6), while above indices for concentrations are not very useful. Hyperspectral reflectance at NIR and SWIR is also useful for non-destructive estimation of leaf water content (Inoue et al., 1993).
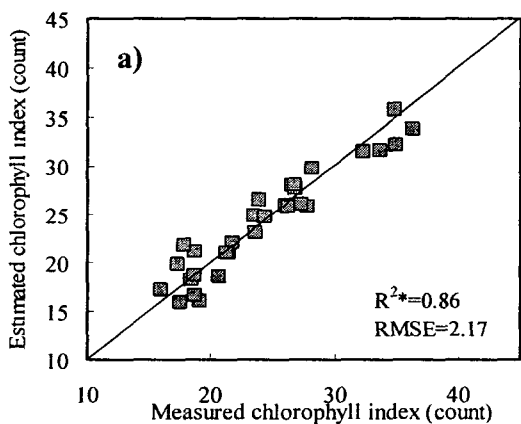
Fig. 3. Hyperspectral estimation of chlorophyll concentrations of rice leaves based on multiple linear regression models. (Inoue et al., 2001)
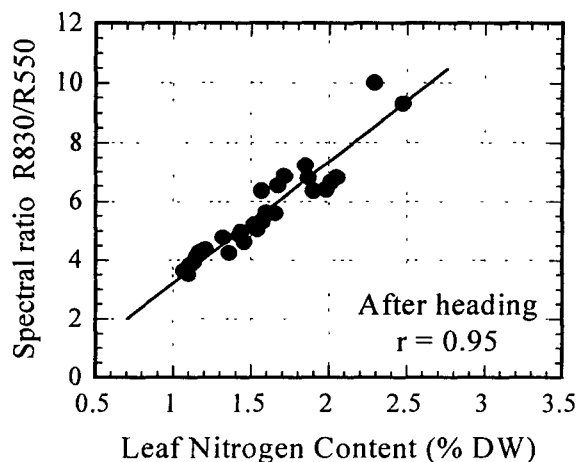
Fig. 4. Relationship between spectral ratio $\rho830/\rho550$ and leaf nitrogen content in rice canopies (Inoue et al., 1998).

2.2.3 Water stress

Canopy surface temperature is quite useful for estimating crop water stress and crop water use; the CWSI is the well-known index for operational irrigation management (Jackson, et al., 1982; Moran et al., 1994; Inoue at al., 1997; Inoue and Olioso, 2004a). A number of experimental studies have shown that leaf or canopy temperature has significant relationships with transpiration, stomatal conductance, and photosynthesis (e.g., Inoue et al., 1990). Using infrared thermal imagery, Inoue (1990) clearly demonstrated that canopy temperature responds sensitively to stomatal conductance, transpiration, and photosynthetic rates. The mean surface temperature in the water-stressed canopy was consistently higher than in the non-stressed one, which was closely linked with physiological depression. Remotely sensed infrared temperatures were especially effective for detecting physiological depression and for comparing the physiological status of various canopies on a real-time basis.

Nevertheless, the applicability of canopy temperature alone is limited, because it is also affected by air temperature, solar radiation, vapor pressure deficit, and wind speed. Thus, the first simple approaches for wider applicability involved canopy-air temperature differences, such as stress-degree-days and the crop water stress index (CWSI), which further incorporated the effect of vapor pressure deficit (Jackson et al., 1981). The CWSI was designed to express the degree of water stress (BC/AB in the upper part of Fig. 5) as a number between 0 (no stress) and 1 (severe stress). The operational applicability of CWSI has been evidenced by commercial instruments and
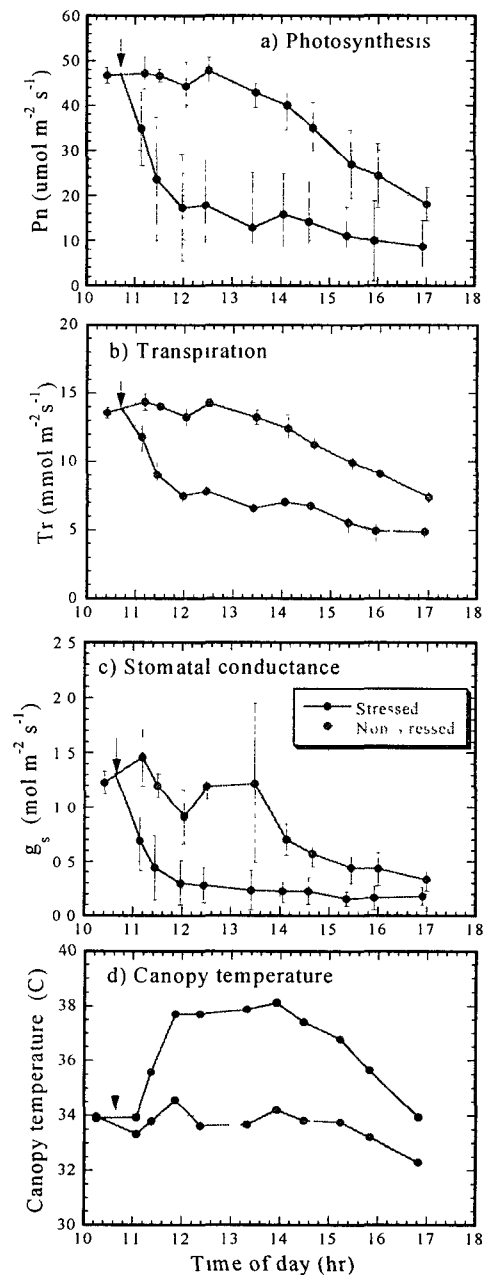

Fig. 10. Physiological status and remotely sensed surface temperature (d) in stressed (●) and non-stressed (○) corn canopies. Arrows in the figure indicate the timing of stress-treatment. (Inoue, 1990)

several application studies using airborne and space-borne thermal imagery (Moran and Jackson, 1991). A simplified approach relating canopy temperature together with a vegetation index to canopy transpiration

(WDI=AC/AB in the lower part of Fig 5) has been proposed for estimating plant stress conditions (Inoue and Moran, 1997; Moran et al, 1994).

2.2.4 Photosynthetic and Transpiration Parameters:

Photosynthetic rate is an important measure of crop productivity The light absorptance of a canopy (fAPAR) and the light use efficiency (LUE) are often used for estimation of crop productivity. We showed the fAPAR can be estimated from optical signatures in VIS, NIR and SWIR (660, 830, 1100, and 1650 nm; Fig. 6), and that the simple vegetation index such as NDVI (= $[\rho830-\rho650]/[\rho830+\rho650]$) may also be used for estimation of the fAPAR (Fig 7) It is an advantage of NDVI that it is simple and commonly measured by many optical sensors, although the accuracy of not very high Figure 9 depicts the within- and between-field variability of daily biomass productivity over the 400 *ha* paddy areas with the resolution of 0.5 m. The imagery was obtained by an airborne imaging system developed by the authors (Inoue et al., 2001). Another interesting approach involves

Fig. 5. Schematic presentation of stress indices based on thermal remote sensing. (Moran & Inoue, 1994).

the use of hyperspectral signatures to estimate photosynthetic activity directly; one such signature is chlorophyll fluorescence, which can be remotely induced and detected (Cecchi et al., 1994; Méthy et al , 1994). Chlorophyll fluorescence in the red and near-infrared regions may be a good indicator of the capacity of photosynthetic electron transport, because fluorescence is emitted mainly from photosystem II (PSII) Yet another approach is to use the spectral reflectance at a wavelength of approximately 530 nm, which is related to both photosynthetic efficiency (photosynthesis/incident photon flux density) and the relative increase of zeaxanthin in the xanthophylls cycle pool (Filella et al., 1996; Peñuelas and Filella, 1998) A high correlation between the normalized reflectance at 531 nm and CO_2 uptake has been found at the canopy scale (Peñuelas and Inoue, 2000). Figure 8 indicates that the LUE can be estimated from $\rho531$
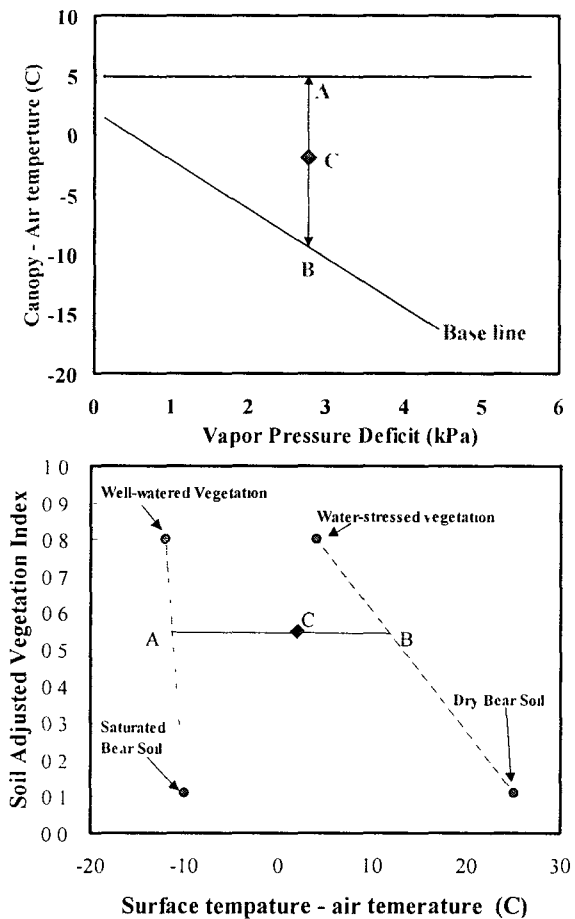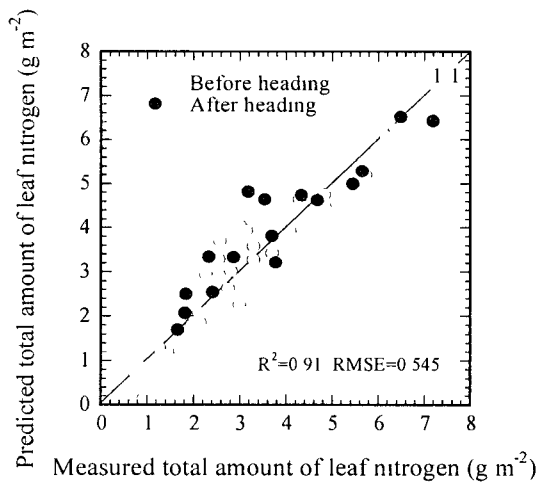
28

Fig. 6. Spectral estimation of nitrogen content of rice canopy based on multiple regression analysis. Reflectance values at 550, 830, 1650, and 2200 nm were used. (Inoue et al., 1998)
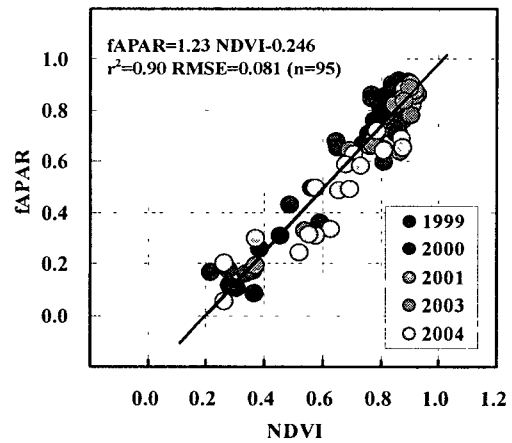

Fig. 7. Relationship between spectral vegetation index (NDVI) and fAPAR of rice canopies. (Inoue et al., 2001)
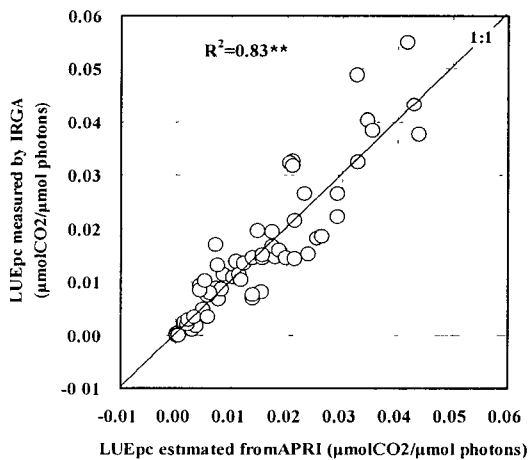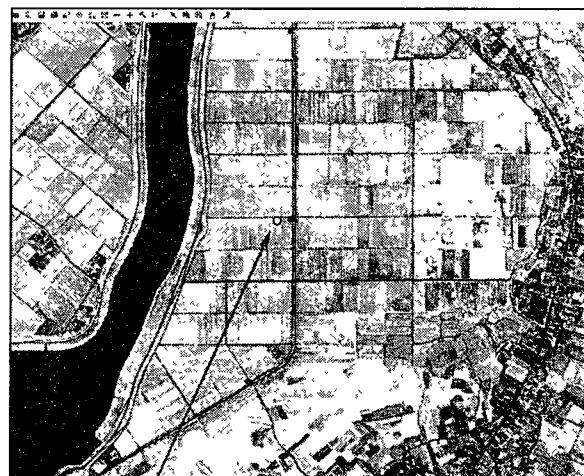

Fig. 8. Comparison between the values of LUE measured and estimated using a spectral index APRI (= [ρ531-ρ570] / [ρ531+ρ570]+0.04). (Inoue and Peñuelas,, 2005)

A tower for CO_2 flux measurement   500m

Fig. 9. Geo-spatial estimation of photosynthetic productivity using airborne multispectral imagery. Notes: 1) The sensing system was developed at NIAES, which covers VSI, NIR, and thermal infrared wavelengths. 2) Spatial resolution on the ground was 0.5m. (Inoue, 2005)

and ρ570 nm (Peñuelas and Inoue, 2000). These relationships can be used for spatial monitoring of crop productivity.

A widely used approach, often using AVHRR data, considers the 'simplified relationship' which was proposed by Seguin and Itier (1983) to relate linearly evapotranspiration to the difference between surface

29

temperature and air temperature. An even simpler type of relation was also derived by Di Bella et al. (2000) over the Argentina Pampa that avoids the use of air temperature. Other combinations of remotely sensed information and process-based modeling are discussed in detail in the next section.

2.2.5 Soil properties and water condition

Radiometric measurements of bare soils are useful to directly extract information about soil surface conditions. Surface reflectance information has been related directly to variability in loess thickness (Milfred and Kiefer, 1976), soil organic matter (Robert, 1993; Zheng and Schreier, 1988), soil calcium carbonate content (Leone et al., 1995), soil nutrients (particularly those associated with soil texture and drainage) (Thompson and Robert, 1995), iron oxide content (Coleman and Montgomery, 1987), and soil texture classes (with similar responses to water and fertilizer) (King et al., 1995). Soil thermal information has been linked with variations in soil moisture content (Idso et al., 1975) and soil compaction (Burrough et al., 1985). Despite the relations among soil reflectance and soil properties, remotely sensed images are not currently being used to map soil characteristics on a routine basis (with the exception of high and medium altitude aerial photographs that serve as base maps in county level soil surveys). This is because the reflectance characteristics of the desired soil properties (e.g., organic matter, texture, iron content) are often confused by variability in soil moisture content, surface roughness, climate factors, solar zenith angle, and view angle. This is particularly true for mapping agricultural soils with varying cultivation practices. In fact, Leek and Solberg (1995) showed that images of surface reflectance acquired during times of greatest plowing activity could be used to map tillage and assist in erosion control.

Salisbury and D'Aria (1992) reported that thermal infrared band ratios from the upcoming EOS ASTER sensor (range 8-14 pm, resolution 90 m) could be used to discriminate such soil properties as particle size, soil moisture, soil organic content, and the presence of abundant minerals other than quartz. Verma et al. (1994) found that better results (particularly for discrimination of the similar reflectance properties of salt-affected soils and normal sandy soils) could be obtained by combining reflectance and temperature information. Wiegand et al. (1986) have used soil and plant samples, videography or SPOT HRV spectral observations, and unsupervised classification to map soil salinity and yield at salt-affected cropped fields. For both crop and soil mapping, remotely sensed images should also be considered for revision of maps of "seasonally-stable" management units. By comparing such maps acquired at optimum times within the season (when soils are bare or when crops cover or phenology is optimum), it may be possible to revise management units midseason in response to unexpected changes. The revision process could be as simple as splaying the remote sensing data as a backdrop to a vector map of management units within a GIS and visually assessing differences (Chagarlamudi and Plunkett, 1993). Multispectral images

obtained when soils are bare could be used to map soil types relevant to precision farming. Maps of spectral variability (obtained under conditions of either bare soil or full crop cover) may prove useful for revision of maps of management units.

The backscattering signals of SAR sensors in long wave-lengths (e.g., C-band at 5.7 cm or L-band at 21 cm) have been used to map soil moisture content of agricultural fields based on a simple linear correlation. This direct relation can be strong for bare soil conditions, but there is considerable scatter when fields of variable crop biomass are included in the regression (Benallegue et al., 1994). Thus, most recent works in mapping within-field soil moisture conditions are based on the use of dual frequency SAR where the combination of long and short (e.g., Ku-band at 2 cm or X-band at 3 cm) wavelengths is used to determine the vegetation-induced attenuation of the long-wavelength signal to improve estimates of soil moisture (Taconet et al., 1994; Prevot et al., 1993; Paloscia et al., 1993; Moran et al., 1997a). The SAR signal is sensitive not only to soil moisture but also to surface roughness (like that associated with differentially tilled agricultural soils) and topography. Engman and Chauhan (1995) suggested that the best application of existing, unifrequency SAR sensors may be for monitoring the temporal change of soil moisture to minimize the influence of variability in roughness, vegetation and topography. Others have suggested that SAR radiative transfer models could be used, with ancillary data provided by remote sensing of non-SAR wavelengths or other sources, to reduce the surface-induced "noise" in the SAR signal and improve soil moisture estimates (Moran et al., 1997b; Wigneron et al., 1995).

2.2.6 Weed

For precision management of pre-planting applications of herbicides, simple information on the presence or absence of plants can be useful, which are provided by simple remote sensors such as the tractor-based sensors (e.g., Richardson et al.,1985). In fact, since perennial weeds tend to remain in the same location each year, there is even the possibility of using the previous year's weed map for pre-plant control decisions (Brown and Steckler, 1995). Management of post-emergence herbicide applications poses more difficulty because it requires discrimination between weeds and crops. This is generally accomplished based on the differences in the visible/NIR spectral signatures of crops and specific weeds (Brown et al., 1994) or by acquiring images at specific times during the season when weed coloring is particularly distinctive (i.e., during flowering). An example of an integrated system for management of weeds with remote sensing input was presented by Brown and Steckler (1995). Their system combined image-derived weed maps with a GIS-based decision model to determine optimum herbicide mix and application rates for no-till corn and resulted in reductions of herbicide use by more than 40%.

2.2.7 Disease and insect infestation

Remote sensing has some potential for detecting and identifying crop diseases. Toler et al. (1981) used false color IR photography to detect Phymatotrichum root rot of cotton and wheat stem rust. In fungal and mildew infected leaves, changes in remotely sensed reflectance have been detected before symptoms were visible to the human eye (Malthus and Madeira, 1993; Lorenzen and Jensen, 1989). Though wide visible and near-infrared bands may be helpful for discriminating healthy and diseased crops (due to changes in foliage density, leaf area, leaf angles, or canopy structure), the best results for identifying diseases were obtained with hyperspectral information in the visible and near-infrared spectrum. Discrimination of diseases may be possible with knowledge of the physiological effect of the disease on leaf and canopy elements. For example, necrotic diseases can cause a darkening of leaves in the visible spectrum and a cell collapse that would decrease near-infrared reflectance. Chlorosis inducing diseases (mildews and some virus) cause marked changes in the visible reflectance (similar to N deficiency) and other diseases may be detected by their effects on canopy geometry (wilting or decreases in LAI). As discussed later, hyperspectral data in the visible and NIR wavelengths have potential for discrimination of crop stress caused by N deficiency, crop disease, water stress, chlorosis, and more. Carter (1994) reported that narrow wavebands derived from hyperspectral data could be used to discriminate the cause of plant stress in six plant species due to eight stress agents: competition, herbicide, pathogen, ozone, mychorrhizae, senescence, and dehydration.

Few studies have been reported on the use of remote sensing for directly assessing insect infestation Indirectly, insect damage to plants has been detected through remote sensing of insect habitat (Hugh-Jones et al., 1992), growth and yield of plants (Vogelmann and Rock, 1989), or changes in plant chemistry. Penuelas et al. (1995) found that increasing infestations of mites in apple trees caused a decrease in the leaf chlorophyll concentration and an increase in the carotenoid/chlorophyll a ratio. These chemical changes were detected by hyperspectral reflectance measurements. It is needed to explore useful algorithms for discriminating different affecting agents.

Since the canopy surface temperature is closely linked with transpiration rate (Inoue, 1990; Inoue et al., 1994), disease can be detected (Nilsson, 1991; Yamamoto et al., 1995) or predicted (Chiwaki et al., 2005) using infrared thermal imagery.

3. Synergy of remote sensing and modeling – a new approach for dynamic and systematic assessment/prediction of crop growth –

3.1 Background

The advantage of remote sensing is that signatures over broad electromagnetic domains can be detected on remote/non-destructive, wide-area, or real-time bases, while the issue surrounding is that measurements are usually instantaneous, directional and infrequent, and must be converted to bio-physically meaningful variables. Conversely, the advantage of process modeling is that numerical models can take account of multiple variables, and can provide dynamic simulations as well as predictions under imaginary situations, while the issue is that experimental determination of model parameters and model validation are not easy, and that it is tedious or impossible to gather necessary input data. Hence, one of the most promising approaches for effective monitoring and accurate prediction of plant production processes is the synergy of remote sensing and process models, which can reinforce each other.

3.2 Case studies in the synergy of remote sensing and process-based models

Here, four case studies are presented to show different types of synergy between process-based models and remotely sensed signatures in optical, thermal, and microwave wavelength domains. The remotely sensed signatures microwave and thermal domains are used as input to the process-based models in the former two cases, and used for dynamic parameterization of process-based models in the latter cases.

3.2.1 Simple scattering model linked with microwave backscattering signatures

Since the radar backscatter is not a function of one or two parameters but rather depends upon a wide range of parameters of the vegetation, soil, topography and the radar sensor itself, the physically-based modeling approach would be essential for retrieving plant variables from backscatter signature under a wide range of plant conditions and sensor configurations. Observations from field experiment should also be understood in generalized manner for more universal applications of results. The backscatter coefficient$\sigma 0$ for the whole canopy has been simply expressed by the water cloud model (Attema and Ulaby, 1978), and proved useful in a wide range of crop types and conditions (e.g., Prevot, 1993; Moran et al, 1998).

$$\sigma^0 = 10 \log \{ A \cdot V_1 \cdot \cos\theta (1 - \exp[-2B \cdot V_2 / \cos\theta]) + \sigma^0_{BG} \exp[-2B \cdot V_2 / \cos\theta] \}$$

where, σ^0 = Backscattering coefficient in power units ($m^2 m^{-2}$) for the canopy; θ = the incident angle; V_1 and V_2 = the descriptors of the canopy; A and B = coefficients that depend on canopy type; σ^0_{BG} = the scattering coefficient of the canopy background. For paddy rice, we can assume that the σ^0_{BG} is constant, and presume that both canopy descriptors can be represented by LAI or total fresh weight (TFW); i.e., $V_1 = V_2 = LAI$ or $V_1 = V_2 = TFW$. Figure 11 shows the values of r^2 as an indicator of model fitting in the two

cases that utilized LAI and TFW as the vegetation descriptor. In case of LAI, the C-band was best fitted, followed by the L-band, while the other bands were poorly correlated. The high correlations (r^2=0.95-0.99) found at HH- and cross-polarization in the C-band at 25° to 45° incident angles suggest the high applicability of the simple scattering model to the C-band when LAI is used as the canopy descriptor. In case of TFW, the

Fig. 11. Degree of fitting of the simple backscattering model to measurements. Results are indicated by a coefficient of determination

fit was high in both the L- and C-bands, but was higher in the L-band. Thus, the TFW is a better vegetation descriptor than LAI for lower frequencies (L-band).
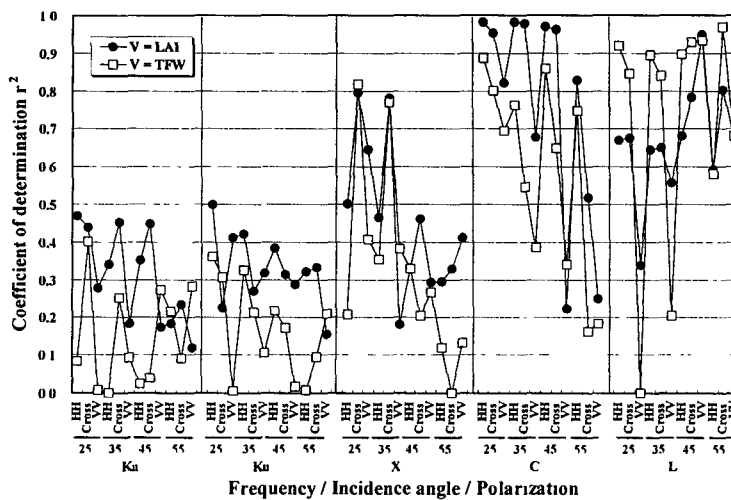
3.2.2 Remote and real-time monitoring of canopy transpiration using a process-based model with remotely-sensed canopy temperatures

The method is based on the energy balance model of a plant canopy, which uses the net radiation absorbed by the canopy and the remotely sensed canopy temperature as key inputs. Measurements were made on drought-stressed, waterlogged, and periodically-irrigated soybean canopies. Canopy transpiration values used for verification of the remote method were calculated from the mean transpiration rates per unit leaf area measured by sap flow gauges. On the basis of the energy balance (Monteith, 1990), canopy transpiration can be expressed as :

$$Tr_c = [Rn_c - \rho Cp (t_c - t_a) ga_h] / \lambda$$

where Tr_c is the canopy transpiration rate, Rn_c is the net radiation absorbed by the canopy, ρ is the density of air, Cp is the heat capacity of air, t_c and t_a are the canopy and air temperatures, ga_h is the aerodynamic conductance for heat, and λ is the latent heat of vaporization.

Canopy transpiration values derived from the remote method are compared with those by the stem flow gauge method from three different aspects: 1) diurnal time course for a particular canopy, 2) one-to-one comparison of ten-minute mean values for all soil water conditions, and 3) daily total values for all soil and meteorological conditions. Figure 12 shows the diurnal course of canopy transpiration values

34

estimated by the two methods. A good agreement was obtained between the two estimates under both cloudy and clear sky conditions for the whole day. There was a good correlation between the direct and remotely-estimated canopy transpiration rates irrespective of the extreme soil water conditions. Similar good correlation was also found in all other days. Comparison of the two methods was made also at a daily basis (Fig.13), since daily total values of canopy transpiration would be practical for irrigation management and ecological studies on natural vegetation. Estimates for all non-stressed and severely-stressed canopies under various climatic conditions were well correlated with each other, the regression line being very close to the 1:1 line. The remote method based on the measurements of canopy surface temperature proved to give the reasonable estimates of canopy transpiration and conductance under a wide range of soil water and micrometeorological conditions. The method will allow continuous measurements of these canopy parameters in the open field with neither plant-sampling nor disturbing the micrometeorological environment of the canopy.
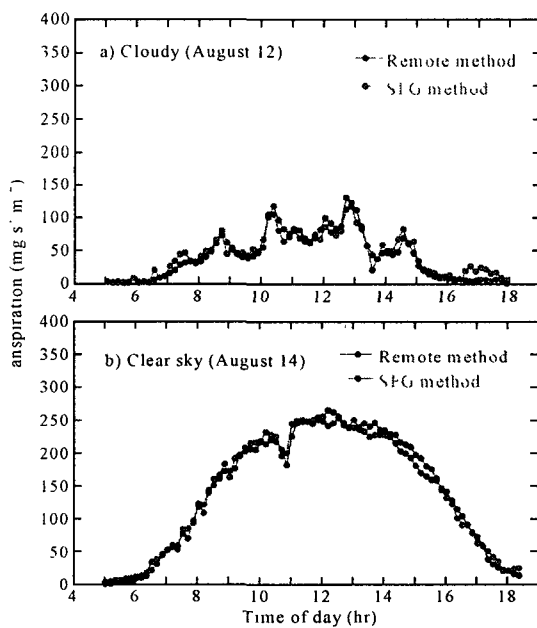

Fig. 12. Diurnal comparison of ten-minute averages of transpiration rates for soybean canopy estimated by remote and stem flow gauge methods under a) cloudy and b) clear sky conditions. (Inoue et al., 1994)
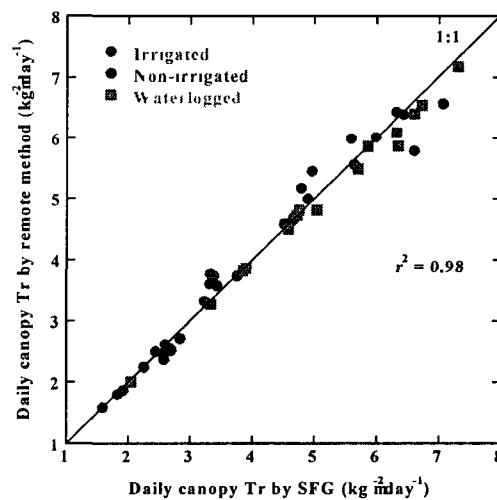
Fig. 13. Comparison of daily transpiration for soybean canopy estimated by remote and stem flow gauge methods. (Inoue et al., 1994)

3.2.3 Dynamic prediction of rice growth based on synergy between remotely-sensed reflectance signatures and a growth model

Spectral reflectance of differentially-managed rice canopies was measured over an entire growing season, and linked with a simple growth model (Inoue et al., 1998). The fraction of absorbed photosynthetically active radiation (fAPAR), which is often used as a key variable in simple process models, was well correlated with spectral vegetation indices. VIs, such as NDVI and SAVI, were derived from the ratio of reflectance at two wavelengths (R660nm and R830nm) and a new VI, termed the normalized difference ND[R1100nm, R660nm], was derived from the difference of R1100nm and R660nm divided by their sum. The use of R1100nm and R1650nm with R660nm and R830nm in multiple regression significantly improved the prediction accuracy of fAPAR (Fig. 6).

The model used here was a simple process model which simulated the growth and yield of irrigated rice based on weather data (Horie, 1985). Dry matter production was expressed as a function of absorbed solar radiation by a canopy and the radiation use efficiency (RUE; the conversion efficiency of radiation to plant dry mass). The absorbed radiation was determined by the incident solar radiation and fAPAR which was a function of LAI. Finally, the grain yield was estimated as a specific proportion (harvest index) of the total dry matter. The model required five initial inputs (date of transplanting, global coordinates of the location, and initial values of dry matter DMi, leaf area index LAIi and developmental index DVIi), and two daily input variables (daily values of incident solar radiation and mean air temperature). Because of this simple input-requirement, it was easily applied where such common weather data are available (Horie, 1993). This model also required twenty five parameters such as variety-specific information (critical daylength for photoperiod-sensitivity, radiation use
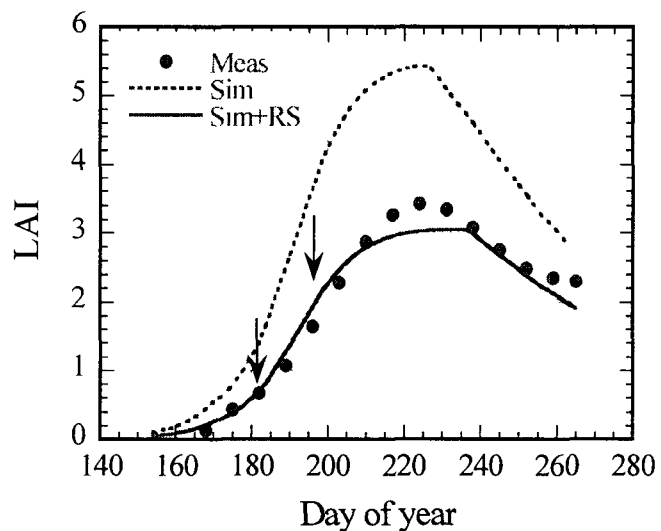

Fig. 14. Prediction of LAI based on the real-time calibration system with remotely sensed fAPAR. Abbreviations Meas, Sim, and Sim+RS mean measured data, simulation only and simulation with remotely sensed data, respectively. Arrows indicate the timing of the data acquisition of remote sensing data. (Inoue et al., 1998)

36

efficiency, extinction coefficient, asymptotic value of LAI when temperature is non-limiting, maximum harvest index, critical temperature for cooling damage, etc.) and some empirical constants for each equation. All parameters were determined for each variety and location based on a large number of field experiments and destructive sampling. The most sensitive crop parameters were found to be those related to phenology, radiation use efficiency, and two initial values (DVIi and LAIi), so that careful specification was needed for the values of those parameters.

A real-time recalibration module based on a simplex algorithm was developed and proved effective in linking the remotely-sensed fAPAR with a simple model. This approach was also useful for inferring the physiological parameters such as radiation use efficiency for each rice canopy without destructive sampling The re-parameterization and/or re-initialization with remotely-sensed information were demonstrated to be a practical and effective approach, especially for operational purposes. The performance of the real-time calibration module was tested using remotely sensed fAPAR values. Prediction results by the simulation model with and without remote sensing inputs are shown in Fig. 14. In this example, remotely sensed data on two dates were used for recalibration. The approach of within-season calibration was undoubtedly effective since a model can be modified to fit reality with the data from the real object no matter what kind of data are used (e.g., estimated by destructive sampling or from remote sensing). With increasing number of remote sensing data used, the simulation curve approached to the reality. The use of fAPAR may be somewhat unique for remote sensing because fAPAR is more closely linked with remotely sensed spectral reflectance than such as LAI and biomass, and a direct measurement of fAPAR is not easy, especially during the ripening period (Inoue and Iwasaki, 1991). Another useful aspect of the within-season calibration of a model with remotely sensed data is that it can provide the realistic estimates of physiological parameters incorporated in the model without any direct measurements. These physiological parameters may be used for field-to-field comparison of productivity or variety-screening. The combination of remotely sensed data and a simple growth model may be useful in improving the accuracy of model prediction and in providing physiological parameters without tedious sampling.

3.2.4 Predicting dynamic change of canopy CO_2 flux based on synergy of remotely sensed data and a SVAT Model

The objective of this study was to investigate the potential of synergy between biophysical/ecophysiological models and remote sensing for the dynamic estimation of biomass and net ecosystem exchange of CO_2 (NEE_{CO2}). We obtained a long-term dataset of micrometeorological, plant,

and remote sensing measurements over well-managed uniform agricultural fields (Inoue et al., 2004). The NEE_{CO2} was measured using the eddy covariance method (ECM), and remote sensing signatures were obtained using optical and thermal sensors. A soil-vegetation-atmosphere transfer (SVAT) model (Calvet et al., 1998) was linked with remotely sensed signatures for the dynamic simulation of CO_2 and water fluxes, as well as biomass, photosynthesis, surface temperatures, and other parameters. This model solves the surface energy balance and the soil water balance at a 5-min time step. The main surface variables simulated by the model are surface temperature, soil moisture in the root zone, surface soil moisture, and energy fluxes. The model requires meteorological variables, albedo, minimum stomatal resistance, LAI, vegetation height, soil texture, wilting point, and field capacity. The model was calibrated and validated
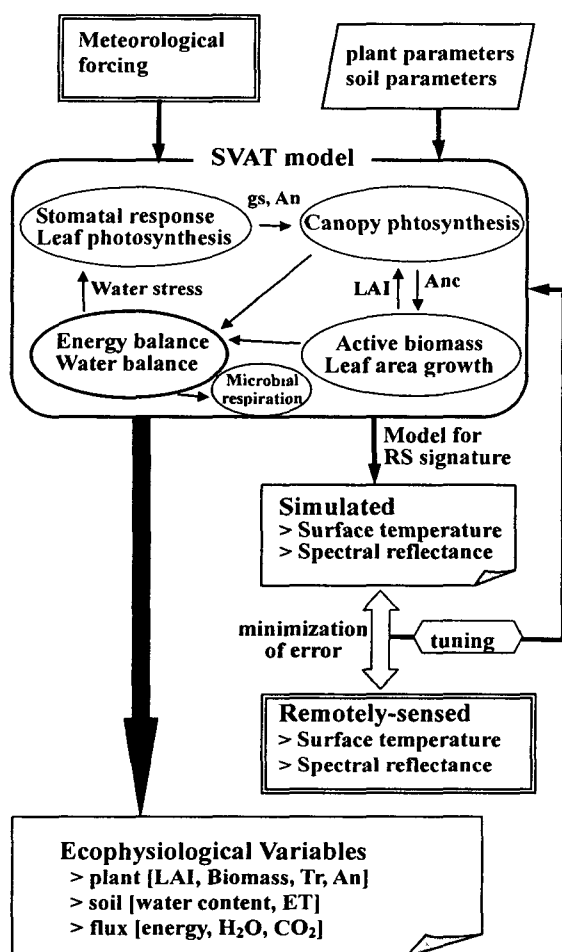

Fig. 15. Structure of the SVAT model and the procedure for parameterization of the model using remotely sensed signature. The final output results (bottom) can be derived through iterative optimization of parameters or state variables. LAI: leaf area index, g_s; stomatal conductance, A_n: leaf net photosynthesis, A_{nc}; canopy net photosynthesis, Tr: transpiration, ET: Evapotranspiration, RS: remote sensing. (Inoue and Olioso, 2004b)
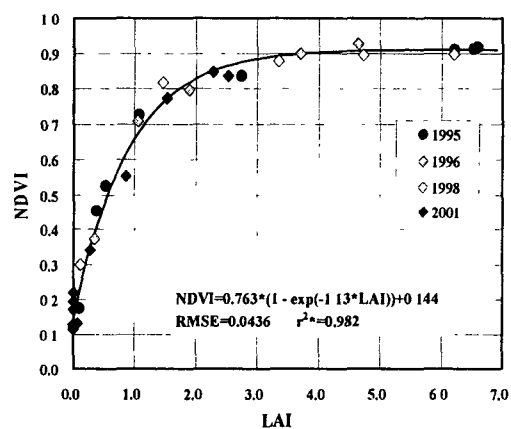

Fig. 16. Relationship between leaf area index LAI and spectral vegetation index NDVI in soybean canopies derived from measurements in the four years: 1995, 1996, 1998 and 2001. Note: r^2* indicates the coefficient of determination adjusted for degree of freedom. (Inoue and Olioso, 2004b)

38

using an 8-year dataset, and the performance of the model was excellent when all necessary input data and parameters were available. However, simulations using the model alone were subject to great uncertainty when some of the important data/parameters such as soil water content were unavailable. Dynamic parameterization of the SVAT model using remotely sensed information (Fig. 15) allows us to infer the target parameters within the model or unknown inputs for the model thorough iterative optimization procedures. A robust relationship between the leaf area index (LAI) and the normalized difference vegetation index (NDVI) was derived and used for dynamic parameterization (Fig. 16).

Our results showed that simulated biomass and NEE_{CO2} agreed well with those measured using destructive sampling and the ECM, respectively. Remotely sensed information can greatly reduce the uncertainty of simulation models by compensating for insufficient availability of data or parameters. This synergistic approach allows the effective use of infrequent and multi-source remote sensing data for estimating important ecosystem variables such as biomass growth and ecosystem CO_2 flux (Fig. 17).
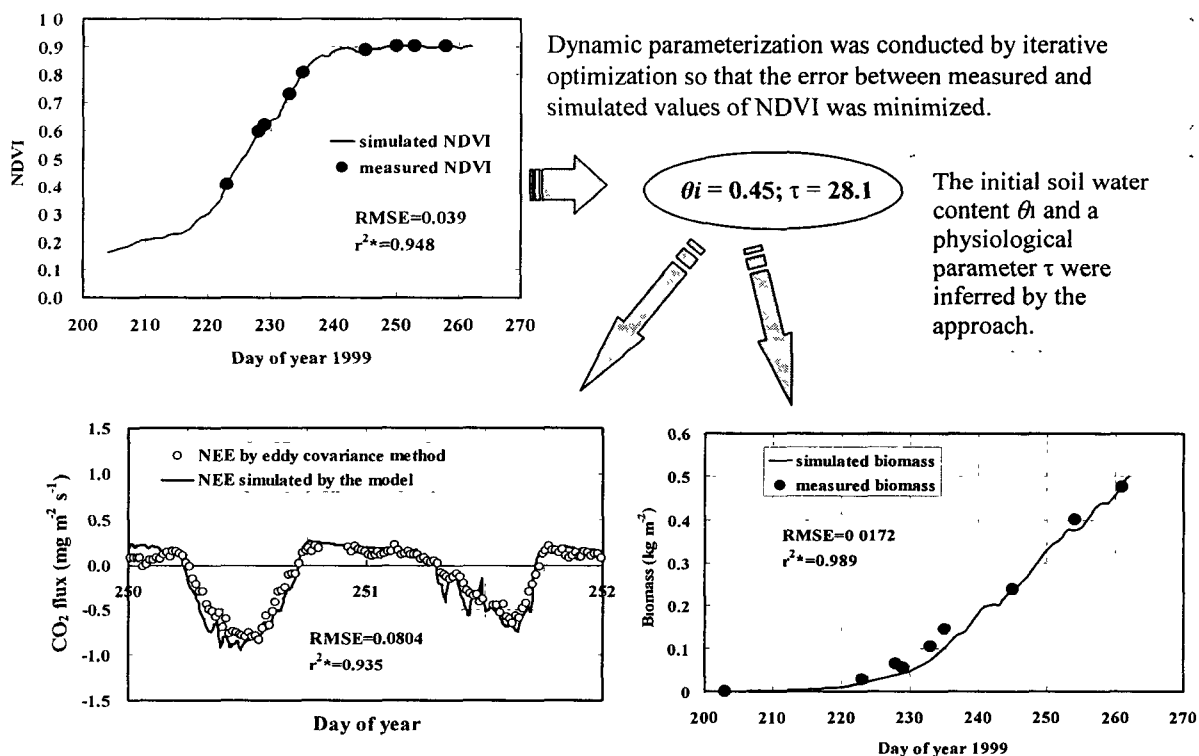

Fig. 17. Dynamic change of ecosystem CO_2 flux, biomass estimated by the synergy of remote sensing and the process model. Note: NEE_{CO2}: net ecosystem exchange. (Inoue and Olioso 2004b)

4. Geo-spatial integration and analysis of static and dynamic information on agro-ecosystems

The objective of this study was to develop a generic geo-spatial simulator for a range of agro-environmental applications. The system was applied to assessment of the fertilized nitrogen to the quality of groundwater.

In general, all GISs have four basic components: (1) a data input subsystem to integrate spatial and descriptive data from a wide range of data sources such as maps, remotely sensed images, and historical archives; (2) a database management subsystem to handle, process, and organize the database; (3) an analyzing subsystem to extract useful information from the data layers; and (4) an output subsystem to present results as maps and documents (Coulson et al., 1991). The input system can store spatial data as raster or vector layers. The analyzing system can execute numerical processing including regressions, correlations, and simulations. The output system often provides visualized products such as 3-D graphics or animations, which allow easy interpretation for scientists, planners, and policy makers.

4.1 The structure and performance of the Geo-Spatial Agro-ecosystem Simulator

Taking account of the above functions, we designed a generic geo-information system for agro-ecosystems that cover the entire farmland in Japan (GSAS). Agricultural farmlands all over Japan have been expressed by farmland parcels with a size of a few *ha*, the total number of which is about 5 millions. Figure 1 depicts the structure of the GSAS. Data integrated in the system include 1) general background map elements such as traffic networks, city boundary, and facilities, etc., 2) topographic data such as elevation, slope, aspect, global position, and soil property, 3) meteorological data such as precipitation, temperature, and snow, 4) information on land types, shape, farm road, irrigation and drainage conditions, and land reformation, 5) accurate acreages of paddy, upland, and the parcel. These data are from different sources including those from Ministry of Agriculture, Forestry and Fisheries. Data from national and local statistics on cropping and land-use, etc. are also superimposed into the system. Data from satellite imagery is also taken into the system and analyzed together with the other data. Any of point measurements can be installed with position data onto the system. Figure 19 depicts an overview of the data system with an example for the central Japan.

One of the most unique points of GSAS is that a small size of farmland is used as the basic unit for integration and other data processing Each parcel is defined basically as a piece of farmland of about 2 *ha* The borderline polygon of each parcel is derived by tracing the border of one or a set of a few individual farmlands. Therefore, all parcels consist of only agricultural land, excluding any of the other land-use such as housing area, road, river, and woodland. Each parcel is given with a unique ID number all over Japan.
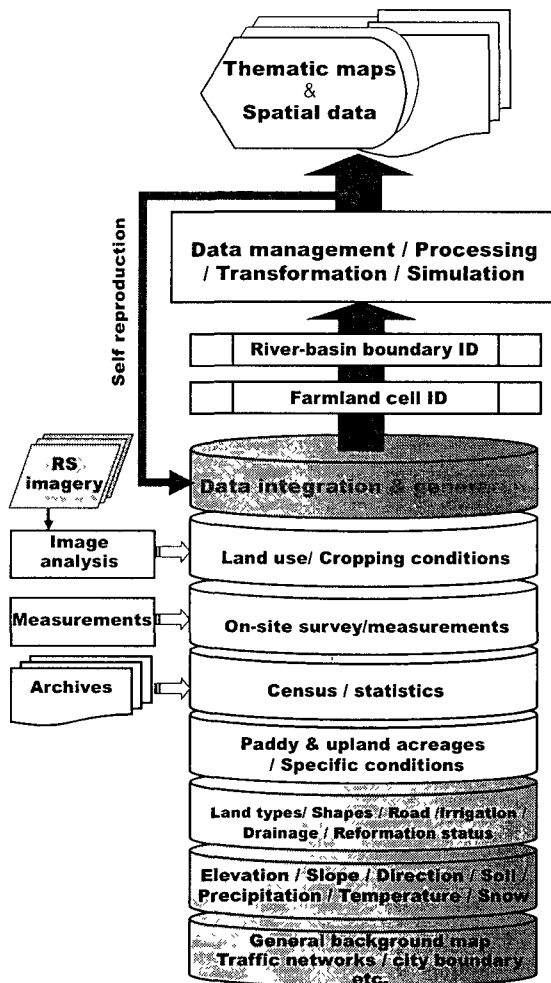

Fig. 18. A Geo-spatial Agro-Ecosystem Simulator: GSAS designed for data integration, analysis and simulation of agro-ecosystem behavior. Notes: 1) The size of unit parcel is basically a few *ha*, where all data are installed in. 2) All farmland parcels over the entire Japan are given with unique ID number. 3) RS: remote sensing. (Inoue at al., 2005)
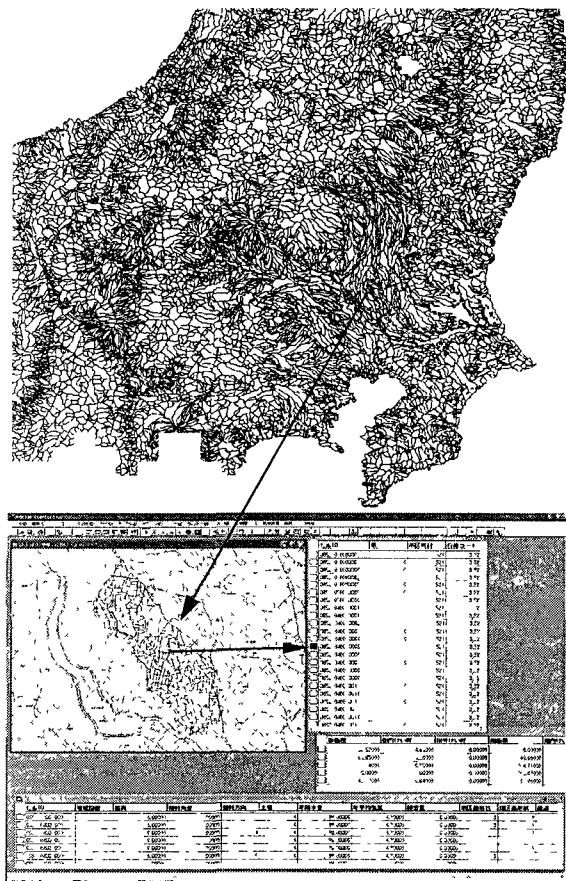
Fig. 19. An overview of the data-system in the GSAS; a range of data, polygons of farmland parcels and river-basin borders are schematically shown. Notes: 1) The upper figure shows the polygons of river-basin boundary. 2) The lower depicts one of the river-basin polygons together with polygons of the parcel units. 3) This example is for the central part of Japan. (Inoue at al., 2005)
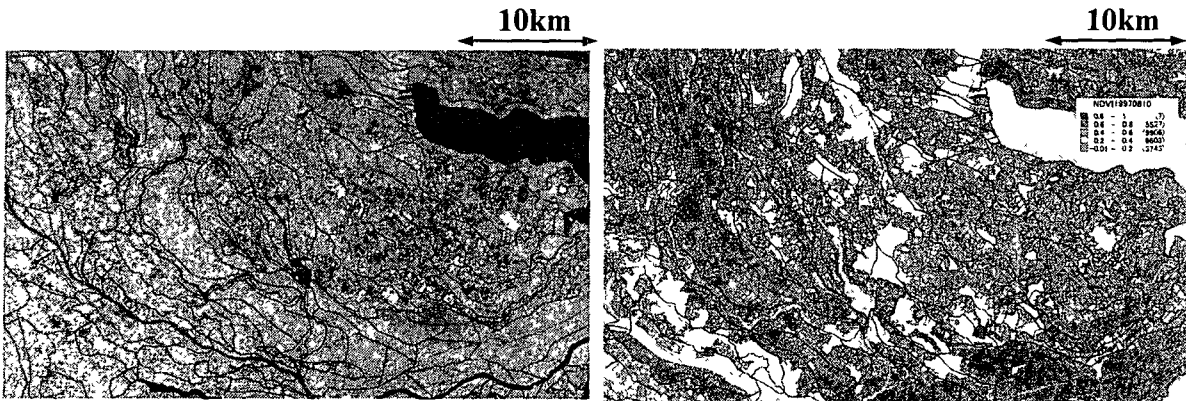
41

Fig. 20. Integration of satellite-derived vegetation conditions at the parcel basis. Note: The left figure is the multi-layered presentation of spectral images (green/red/near-infrared; satellite SPOT) superimposed over the polygons of river-basin and farmland parcels. The right shows the spectral vegetation index calculated and stacked at the parcel basis in the GSAS. (Inoue at al., 2005)

Another important layer is one for the boundaries of river-basins. The upper part in Fig. 19 shows the polygons of river-basin boundaries, one of which is zoomed up in the lower left of the figure. The small polygons within the river-basin boundary are the unit parcels. Attached tables show some of attribute data for each parcel. Thus, the GSAS enables us to extract any of necessary parcels by ID#, attributes, and/or by river-basin boundary, administrative boundary, or a boundary of arbitrary shape/ size on the display over the entire Japan.

Figure 20 depicts the use of satellite image with the GSAS. This example shows the processing and installation of vegetation index NDVI (= $[\rho_{NIR}-\rho_{RED}]/[\rho_{NIR}+\rho_{RED}]$; ρ_{NIR} and ρ_{RED} are reflectance at near-infrared and red wavelengths) onto the system. The upper figure shows the multi-layered images of green, red and near-infrared bands from the satellite SPOT with the polygons of river-basin boundary. The NDVI was calculated from those spectral images at the pixel basis (25 m), and average and variability (e.g., standard deviation within each parcel) of NDVI values were stored as attributes of each parcel. The NDVI, a kind of standard information from satellite imagery, is a useful index for estimating the amount of green vegetation. Any of satellite image data in optical, thermal or microwave wavelengths can be stacked in the similar way.

The GSAS is not only for integration of data, but for searching, extracting, processing, transforming, and calculating any part of the data. Thus, the system is a powerful tool for up- and down-scaling, simulation, and assessment of agro-ecosystem variables. Results from such calculations are also stacked back into the data system, so that the system works as a self-reproductive reactor.

42

4.2 A case study for geo-spatial assessment of groundwater quality as affected by fertilizing

Losses of nutrients from agricultural land can pollute both ground and surface waters and the atmosphere. Therefore, it is strongly required to minimize the impact of agricultural management on environmental pollution (MAFF, 2000). The environmental criterion for the nitrate in groundwater is 10 ppm, but there are a number of evidences that the nitrate concentration greatly exceeds the criterion in many regions in Japan (Nishio, 2005). Besides, it has been pointed that the pollution seems to be closely related to amount of fertilizers applied in the regions (Kumazawa, 1999; Nishio, 2001). Thus, in this case study, we focused on the impact of the fertilizer on nitrate (NO_3) in the groundwater in Ibaraki prefecture. The data of cropping area for all crop species in 1985 and 2000 were taken into the GSAS. The sum of nitrogen that is possibly left in the cropped-land and leaching into the groundwater was integrated at the town scale since the data of nitrate measurements at surveyed wells were publicized only as a statistical summary at the town scale, i.e., percentage number of wells with exceeding concentration of nitrate in
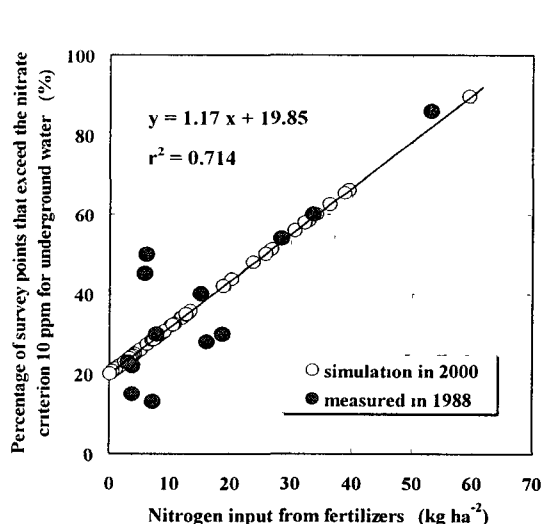

Fig. 21. Relationship between nitrogen input from fertilizers and percentage of wells with excess nitrate concentrations. Notes: 1) The criterion for groundwater nitrate is 10 ppm. 2) The percentage risk in 2000 was simulated using the regression equation derived from the data in 1988 and the actual cropping areas in 2000. (Inoue at al., 2005)
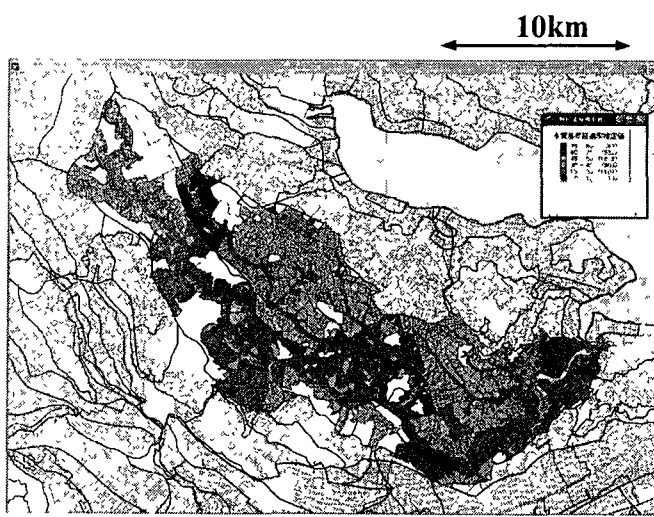
Fig. 22. Regional assessment of percentage risk of excess nitrate concentration in the ground water. Note: The percentage risk is calculated for the entire area of a river-basin at the parcel basis, on the basis of the equation obtained in Figure 4 and the data of cropping area in 1995. (Inoue at al., 2005)

43

each town (Shimada et al., 1989). The nitrogen balance was estimated from the amount of nitrogen applied and used by each crop species using the estimates by Nishio (2001).

Figure 21 shows the relationship between nitrogen load from fertilizers and percentage number of wells with exceeding concentration of nitrate. The nitrogen load (x-axis) was estimated by GSAS while the percentage of wells with excess nitrate concentration (y-axis) was derived from chemical analysis of well water in 1988. It is obvious that these two are highly correlated (r^2=0.71), which strongly indicate the impact of nitrogen load from fertilizer on the groundwater quality. The "simulation in 2000" indicates the percentage number of wells with excess nitrate concentration in 2000 based on simulation using the above regression model and the cropping data in 2000. Results suggest that there are still a number of areas with high risk of excess nitrate concentration in 2000. This simulation was done assuming the unit load for each crop species did not have changed from 1988 to 2000, but less use of fertilizer and/or improvement of application method might have decreased the risk. Nevertheless, considering the effects of such technical improvement and the range of risk (up to 90%) in Figure 21, the risk may not be much reduced. More detailed research and assessment are needed using measured data.

On the basis of similar datasets in GSAS, the geo-spatial down-scaling was attempted at the scale of river-basin. Figure 22 depicts the risk of excess nitrate in well water at the parcel basis, which was estimated the regression model and data of cropping areas in 1995. Since agricultural statistics are available only at the administrative boundary (city/town/village) while a river-basin usually covers across many of them, the GSAS was used for down-scaling of nitrogen input to the parcel scale. This case study clearly showed that the GSAS allows this type of geo-spatial analysis at various scales anywhere in Japan

The risk of loss by nitrate leaching can be reduced by precise implementation of appropriate management practices. The rate of nitrogen fertilizer should not be greater than the crop requirement. The nitrogen use efficiency will be increased by timely application of necessary amount of fertilizer based on *in situ* measurements and diagnosis by such as remote sensing (Inoue, 2003). It is also important to take account of the nitrogen available from the soil organic matter, previous crop residues and organic manures. Thus, it is recommended to adopt a systematic approach to fertilizer planning. Accurate records of past fertilizer use and the regular calibration of fertilizer application machinery will increase the accuracy of fertilizer decisions and application. The information system like the GSAS plays an important role in such applications.

5. Conclusions

44

Within-field or between-field differences can be assessed efficiently by remote sensing. Through the review and case studies on the potential/limitations of remote sensing, the synergy of remote sensing and process-based models was suggested to be one the most promising approaches Further experimental and theoretical studies are needed for both scientific and operational applications of the approach. A geo-spatial agro-ecosystem simulator has been developed that enables to integrate and analyze a range of geo-spatial data and information at a basis of farmland parcel. This system has a great potential for various agro-ecosystem applications such as spatial assessment of crop production, impact of agricultural practices on environmental quality, as well as planning of landscape management. It is desirable to improve the structure and function of the system through both experimental and operational case studies.

References

Calvet, J.C , Noihan, J., Roujean, J.L., Bessemoulin, P., Cabelguenne, M., Olioso, A., Wigneron, J.P. 1998. An interactive vegetation SVAT model tested against data from six contrasting sites. *Agricultural and Forest Meteorology*, 92, 73-95.

Chiwaki, K., Nagamori, S., Inoue, Y. 2005. Predicting bacterial wilt disease of tomato plants using remotely sensed thermal imagery *Journal of Agricultural Meteorology*, 24, (in press)

Coulson, R N., Lovelady, C.N., Flamm, R.O , Spradling, S.L., Saunders, M.C. 1991. Intelligent geographic information systems for natural resource management In; *Quantitative Methods in Landscape Ecology* (Eds., Turner, M.G. and Gardner, R.H.), Springer, New York, 138-153.

Inoue, Y. 1990 Remote detection of physiological depression in crop plants with infrared thermal imagery. *Japanese Journal of Crop Science,* 59, 762-768.

Inoue, Y., Kimball, B.A., Jackson, R.D., Pinter, P.J., Jr., Reginato, R.J. 1990. Remote estimation of leaf transpiration rate and stomatal resistance based on infrared thermometry. *Agricultural and Forest Meteorology*, 51, 21-33.

Inoue, Y., Morinaga, S., Shibayama, M. 1993. Non-destructive estimation of water status of intact crop leaves based on spectral reflectance measurements. *Japanese Journal of Crop Science*, 62, 462-469.

Inoue. Y., Sakuratani, T., Shibayama, M., Morinaga, S. 1994. Remote and real-time sensing of canopy transpiration and conductance - comparison of remote and stem flow gauge methods in soybean canopies as affected by soil water status -. *Japanese Journal of Crop Science*, 63, 664-670.

Inoue, Y., Moran, M.S. 1997. A simplified method for remote sensing of daily canopy transpiration - a case study with direct measurements of canopy transpiration in soybean canopies -. *International Journal of Remote Sensing*, 18, pp.139-152.

Inoue, Y. 1998. Application of remote sensing to information-based precision farm management (in Japanese). *Journal of the Japanese Society of Agricultural Machinery*, 60(1), 127-134; (2), 139-146; (3), 141-150.

Inoue, Y , Moran, M.S., Horie, T 1998. Analysis of spectral measurements in rice paddies for predicting rice growth and yield based on a simple crop simulation model. Plant Production Science, 1, 269-279.

Inoue, Y., Morinaga, S., Tomita, A. 2000. A blimp-based remote sensing system for low-altitude monitoring of plant variables: a preliminary experiment for agricultural and ecological applications. *International J. of Remote Sensing*, 21, 379-385.

Inoue, Y., Peñuelas, J. 2001. An AOTF-based hyperspectral imaging system for field use in ecophysiological and agricultural applications. *International Journal of Remote Sensing*, 22, 3883-3888.

Inoue, Y., Olioso, A., Moran, M.S., Qi, J., Choi,W. 2001. Remote sensing of photosynthetic capacity of vegetation based on airborne spectral measurements. *Proc 34th Conference of the Remote Sensing Society of Japan*, 239-242.

Inoue, Y., Kurosu, T., Maeno, H., Uratsuka, S., Kozu, T., Dabrowska-Zielinska, K., Qi, J. 2002. Season-long daily measurements of multi-frequency and full-polarization backscatter signatures over paddy-rice field and their relationship with biological variables. *Remote Sensing of Environment,* 81, 194-204.

Inoue, Y. 2003. Synergy of remote sensing and modeling for estimating ecophysiological processes in plant production. *Plant Production Science,* 6, 3-16.

Inoue, Y., Olioso, A., Choi, W. 2004. Dynamic change of CO_2 flux over bare soil field and its relationship with remotely sensed surface temperature. *International Journal of Remote Sensing* 25, 1881-1892.

Inoue, Y., Olioso, A. 2004a. Synergistic linkage between remote sensing and biophysical models for estimating plant ecophysiological processes. *Journal of Japanese Society of Remote Sensing,* 24, 1-17.

Inoue, Y., Olioso, A. 2004b. Estimating dynamics of CO_2 flux in agro-ecosystems based on synergy of remote sensing and process modeling –a methodological study-. In: *Global Environmental Change in the Ocean and on Land* (Eds, Shiyomi,M. et al.), Terrapub, 375-390.

Inoue, Y., Peñuelas, J. 2005. Relationship between light use efficiency and photochemical reflectance index in soybean leaves as affected by soil water condition. *International Journal of Remote Sensing,* 26, (in press).

Inoue, Y., Dabrowska-Zierinska.K., Qi, J. 2005. A geo-spatial agro-ecosystem simulator for agro-environmental assessment and managements. *Proc 1st Asian Conference of Precision Agriculture,* (in press).

Kumazawa, K. 1999. Present status of nitrate pollution in groundwater. *Japanese Journal of Soil Science and Plant Nutrition,* 70,207-213. *(in Japanese)*

MAFF, UK. 2000. *Fertilizer Recommendations for Agricultural and Horticultural crops (RB209).* 7th Edn., 1-175.

Moran M. S., Clarke, T.R., Inoue, Y., Vidal, A. 1994. Estimating crop water deficit using the relation between surface-air temperature and spectral vegetation index. *Remote Sensing of Environment,* 49, 246-263.

Moran, M.S., Inoue, Y., Barnes, E.M. 1997. Opportunities and limitations for image-based remote sensing in precision crop management. *Remote Sensing of Environment,* 61, 319-346.

Nishio, M. 2001. A method to assess the risk of nitrate pollution of groundwater by the nitrogen fertilization load from the individual crop species. *Japanese Journal of Soil Science and Plant Nutrition,* 72, 522-528 *(in Japanese)*

Nishio, M. 2005: Agriculture and Environmental Pollution - Technology and Policy for Soil Environment -. Rural Culture Association, Tokyo. *(in Japanese)*

Peñuelas, J., Inoue, Y. 2000. Reflectance assessment of canopy CO_2 uptake. *International Journal of Remote Sensing,* 21: 3353-3356.

Shimada, M., Takahashi, G., Oyamada, N., Kobayashi, T., Suzuki, Y. 1989. Research of water quality of well water in Ibaraki prefecture. *Annual Report of Ibaraki Prefectural Institute of Public Health,* 27, 48-55.

* Some of references cited in the text are not listed in this section, but can be found in Inoue (2003) or Inoue and Olioso (2004b).